A Mossbauer study of paramagnetic and magnetic components in an uncalcined iron manganese oxide powder

1990 J. Phys.: Condens. Matter 2 3391

(http://iopscience.iop.org/0953-8984/2/14/023)

J. Phys.: Condens. Matter **2** (1990) 3391–3398. Printed in the UK

A Mössbauer study of paramagnetic and magnetic components in an uncalcined iron manganese oxide powder

Haydée le Roux

Condensed Matter Physics Research Group, Department of Physics, University of the Witwatersrand, PO WITS 2050, South Africa

Received 1 August 1989

Abstract. Using Mössbauer effect (ME) spectroscopy and powder x-ray diffraction an uncalcined iron manganese oxide catalytic precursor was examined at room temperature after a magnetic separation of the magnetic and paramagnetic components was made. A previous identification of the paramagnetic component as the γ-$FeMnO_3$ defect spinel is confirmed. Its interplanar spacings have now been measured and they show a strong resemblance to the γ-Fe_2O_3 defect spinel. Both defect spinels give rise to similar mixed indices indicating a non-FCC structure. The previously postulated γ-$Mn_{0.16}Fe_{1.84}O_3$ magnetic defect spinel could not be confirmed. The magnetic component is now compared with a synthetic magnetite. The ME parameters are strikingly similar and the x-ray spectrum of the magnetic fraction exhibits predominantly magnetite-like rings. Furthermore the quadrupole splitting observed in the Mössbauer spectrum of this phase is very small, confirming normal spinel behaviour. It is now postulated that the magnetic spinel is a Mn-substituted magnetite with the approximate composition $Mn_{0.6}Fe_{2.4}O_4$. Both phases have the same lattice parameter $a = 0.844$ nm calculated on the assumption of cubic structures.

1. Introduction

Evidence of a new structural phase that forms in co-precipitated iron manganese oxide powders obtained from Mössbauer effect (ME) spectroscopy was presented recently [1]. This phase is a paramagnetic defect spinel with the formula γ-$FeMnO_3$ where the Fe and Mn contents are very nearly equal. It occurs in Fe–Mn–O powders with an Fe:Mn ratio of 62:38 calcined below 500 °C, as well as in uncalcined powders. Its presence is associated with a magnetic component that was also identified as a defect spinel, γ-$Mn_yFe_{2-y}O_3$ with $y \simeq 0.16$.

The same ME spectrum was observed in a co-precipitated, uncalcined, Fe–Mn–O powder with a slightly different Fe : Mn ratio of 59 : 41. These two powders are assumed to be similar. The latter powder was investigated further to obtain information on the structures of the paramagnetic and magnetic components present in both powders.

Measurements of Debye–Scherrer powder patterns made on co-precipitated 59Fe–41Mn–O revealed several reflections with mixed odd and even indices, [2]. In addition reflections resembling those of magnetite were present. This pattern is similar to that of the defect spinel, γ–Fe_2O_3 ($a = 0.833$ nm) [3]. The presence of mixed indices, forbidden by space group extinction for FCC structures, implied that the structure was no longer

0953-8984/90/143391 + 08 $03.50

FCC [4]. These x-ray data confirmed that a defect spinel is present in the 59Fe–41Mn–O powder but were insufficient to enable an identification of two different defect spinels to be made.

The quadrupole splittings determined from ME spectra are large for the two doublets in the paramagnetic spinel implying asymmetrically occupied Fe with neighbouring Mn sites in this phase. The almost zero quadrupole splitting for the magnetic component suggests that this is a normal FCC spinel. To achieve clarification, a magnetic separation of the powder was made and the separated fractions were examined.

As much of this work revolves around the structure of magnetite it is appropriate to comment on this compound. Natural magnetite is an inverse spinel ferrite with a formula usually written as $(Fe^{3+})[Fe^{2+}Fe^{3+}]O_4$ where the round brackets refer to tetrahedral (A) sites and square brackets to octahedral (B) sites. The ferrous and ferric ions in octahedral sites are equal in number. Although ferrous and ferric sites are usually easily distinguished in ME spectra, the magnetite spectra are an exception. Magnetite has been shown by Verwey and Haayman [5] to undergo a structural transition (from FCC to orthorhombic) at about 120 K which results in a metal-to-insulator transition. Verwey and Haayman postulated a fast-electron-transfer (electron hopping) process in the octahedral sites between ferrous and ferric ions above this temperature. This has the effect of averaging out the spectrum and cancelling any quadrupole splitting.

Manganese ferrites have been widely used in electronics and their properties are known to be strongly affected by the method of preparation. These ferrites have been studied more extensively after calcination above 600 °C than below this temperature. More recently use of these oxides as catalysts in fuel synthesis by the Fischer–Tropsch process have reportedly resulted in improved catalytic performances.

2. Experimental details

2.1. Sample preparation and magnetic separation

Two uncalcined powders were made by continuous co-precipitation [6]. The proportion of iron to manganese was kept as close to 60:40 at.% as possible being 62:38 in one powder and 59:41 in the other. A mixed solution of 0.15 M iron (III) nitrate (Merck, pa) and 0.15 M manganese (II) nitrate (Merck, pa) was used with 11 wt% ammonium hydroxide (Merck, pa) as precipitating agent. During the precipitation the temperature was kept at 70 °C and the pH value at 8.2. To prevent premature hydrolysis, the acidity of the iron nitrate solution was increased with concentrated nitric acid. The mean residence time of the suspension in the mixing vessel was about 20 s. The precipitate was continuously filtered in approximately 25 g batches, thoroughly washed with hot, deionised water and oven dried at 120 °C.

The results obtained for the powder with 62Fe–38Mn–O have been reported [1]. The powder with 59Fe–41Mn–O has been investigated by ME spectroscopy and by Debye–Scherrer powder diffraction before and after a magnetic separation was made.

The magnetic separation was made using a bar magnet and a Petri dish. About 2 g of powder, taken from the available stock, was placed in the Petri dish. Holding one end of the bar magnet against the base of the dish the powder, which then resembled iron filings, was held in position. On tilting the base of the dish and agitating the powder with the magnet, paramagnetic grains could escape, slide down the incline and be collected at the rim of the dish. Two interim ME spectra were measured on the magnetic fraction

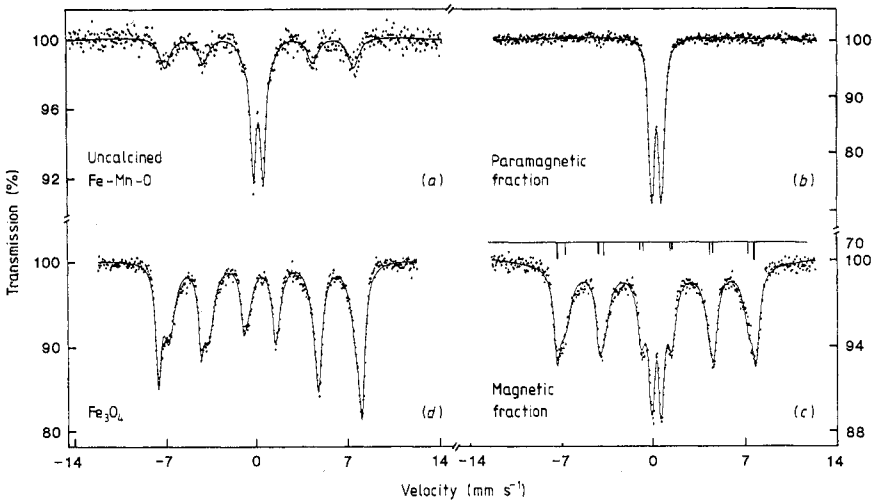

Figure 1. Mössbauer spectra of uncalcined 59Fe–41Mn–oxide powders: (*a*) the spectrum before magnetic separation; (*b*) the paramagnetic fraction after magnetic separation; (*c*) the magnetic fraction after magnetic separation; and (*d*) the spectrum for synthetic magnetite, Fe_3O_4. The subspectra in (*c*) are shown by the stick diagram where A sites are represented by thick sticks and B sites by thin sticks. Intensities are approximately proportional to the lengths of the sticks.

to determine the degree of separation after which the process was repeated until a final ME spectrum could be recorded at room temperature. A small amount of the paramagnetic phase was retained in the magnetic fraction but the separation of the paramagnetic phase itself was very nearly complete.

After separation new samples were mounted for ME spectroscopy. The quantity of powder in each sample was determined in the usual way by the background-to-sample-count-rate ratio. There were thus three independently prepared samples: the unseparated powder and two separated components.

A synthetic magnetite (technical grade), Fe_3O_4, made by BDH Chemicals, was examined at the same time to check for similarities between two synthetic materials.

2.2. The Mössbauer spectra and x-ray diffraction

The ME spectra of these powders were measured at room temperature in conventional transmission geometry using a Co(Rh) source. The spectrometer, source and curve fitting procedure have been described previously [1].

Debye–Scherrer powder patterns were measured on all three samples.

3. Results

The ME spectrum of the two components in the unseparated uncalcined powder is shown in figure 1(*a*). The separation of the paramagnetic phase, figure 1(*b*), is estimated to be 97% complete. Although the magnetic fraction retained some of the paramagnetic phase after separation, figure 1(*c*), its concentration was sufficiently increased for greater

Table 1. (*a*) Hyperfine ME parameters for the paramagnetic fraction. (*b*) Hyperfine ME parameters for the magnetic fraction and synthetic magnetite.

(*a*)		Uncalcined Fe–Mn–O powder	Paramagnetic fraction	From [1]
Doublet (1)	δ(Fe) (mm s^{-1})	0.32(3)	0.34(1)	0.34(1)
	ΔE (mm s^{-1})	0.55(6)	0.60(1)	0.69(2)
	Γ (mm s^{-1})	0.39(5)	0.42(1)	—
Doublet (2)	δ(Fe) (mm s^{-1})	0.33(3)	0.33(1)	0.33(2)
	ΔE (mm s^{-1})	0.94(10)	1.04(2)	0.83(4)
	Γ (mm s^{-1})	0.42(1)	0.40(2)	—
(*b*)		Magnetic fraction	Synthetic magnetite	From [1]; A and B sites
Tetrahedral A sites	δ(Fe) (mm s^{-1})	0.33(9)	0.32(1)	0.32(2)
	ΔE (mm s^{-1})	~0	~0	−0.00(2)
	Γ (mm s^{-1})	0.55(5)	0.48(1)	—
	H (T)	46.8(1)	48.6(1)	45.4(2)
Octahedral B sites	δ(Fe) (mm s^{-1})	0.35(1)	0.54(1)	—
	ΔE (mm s^{-1})	~0	~0	—
	Γ (mm s^{-1})	1.01(1)	1.08(3)	—
	H (T)	43.3(3)	44.9(1)	—

precision in the analysis to be achieved. Both A and B sites could be identified. These sites are represented by the stick diagram which shows the A sites (thick sticks), the B sites (thin sticks) and the approximate relative intensities of the subspectra. The synthetic magnetite is shown in figure 1(*d*). The peak intensities in (*a*), (*b*) and (*c*) are not comparable with each other for reasons given in section 2.1.

The hyperfine parameters: the isomer shift δ with respect to Fe; the quadrupole split ΔE ($=\frac{1}{2}e^2qQ$ where eQ is the nuclear quadrupole moment, eq the electric field gradient at the nuclear site and e the proton charge), the width Γ, all in mm s^{-1}, and the hyperfine field H in T, are listed in table 1(*a*) and (*b*). The equivalent values obtained by Kolk *et al* [1] for the unseparated powder are presented in the last column.

The parameters measured on the paramagnetic fraction, figure 1(*b*), were used to constrain the values of the equivalent parameters of the components in figure 1(*a*) and 1(*c*). This ensured that the magnetic fraction was fitted with minimum interference from its neighbouring phase. In the course of using the least squares fitting programme for the spectrum in figure 1(*c*) it was observed that the two innermost peaks of the sextet were more intense than is usual for randomly distributed particles in powders. It was found, on allowing the programme to free these intensities independently for the two superimposed sextets, that the ratio of the intensities of the inner to the outer pairs of peaks was two-thirds instead of the more usual one-third. Only the octahedral sites were affected. The outer sextet of A sites had the usual intensity ratios. The reason for this behaviour is not understood. The magnetite displayed an identical behaviour. The measured d-values of the separated powder fractions and of synthetic magnetite are listed in table 2. The d-values of magnetite measured by Rooksby [3] and those of γ-Mn_2O_3 reported by Moore *et al* [7] are also listed. The measured d-values of the

Table 2. Lattice spacings of paramagnetic and magnetic fractions, magnetite and γ-manganese oxide

hkl	Paramagnetic fraction (nm)	Int. (est.)	Magnetic fraction (nm)	Int. (est.)	Magnetite (nm)	Int. [3]	γ-Mn_2O_3 (nm)	(int.)
111	0.487	W	0.488	M	0.485	3	0.493	40
200	0.417	M	0.419p	W	—	—		
(202)	0.307	VW	—	—	—	—	0.308	60
220	0.299	VW	0.298	M	0.296	6		
221	0.287	VW	0.287p	VVW	—	—		
300	0.275	W	0.277p	VW	—	—	0.274	70
310	0.264	VW	—	—	—	—		
311	0.255	M	0.254	S	0.253	10		
222	0.248	M	0.248p	W	0.242	1	0.248	100
320	0.236	VVW	0.235p	VVW	—	—	0.239	40
400	0.211	VVW	0.211	M	0.209	5		
322	0.203	VW	0.204p	VW	—	—	0.203	20
422	—	—	0.172	MW	0.171	4		
430	0.170	VVW	0.170p	VVW	—	—		
511	0.627	VVW	0.163	M	0.161	6		
520	0.157	VW	0.157p	VVW	—	—		
521	0.154	VW	0.154p	VVW	—	—		
440	0.149	VW	0.149	S	0.148	7		
433	0.143	VW	0.144p	VVW	—	—		
620	—	—	0.133	D	0.132	1		
533	—	—	0.129	VWD	0.128	3		
444	—	—	0.122	VVW	—	—		
642	—	—	0.113	VWD	0.112	2		
731	—	—	0.110	BD	0.111	5		
800	—	—	0.106	VW	0.105	2		

unseparated powder are a composite of those of the two fractions and are therefore not listed. The lattice parameters of the paramagnetic and magnetic fractions were determined assuming a cubic structure for both components and were found to have the same value of $a = 0.844$ nm.

The x-ray pattern of the paramagnetic phase displayed nearly all the rings seen in the unseparated powder but their intensities were noticeably different. The rings were estimated to have medium to very, very weak intensities with respect to magnetite as given by Rooksby [3]. The weakest intensities, of the forbidden planes, are similar to those reported for γ-Fe_2O_3. The normal FCC reflections are much less intense for the paramagnetic phase than for either the γ-Fe_2O_3 phase or for magnetite.

The powder pattern of the magnetic fraction contained all the rings present in synthetic magnetite and most of the rings in the paramagnetic component including forbidden reflections. The intensities of the latter reflections are much weaker in the pattern of the magnetic fraction than in that of the paramagnetic fraction. Assuming that the loss of intensity is due to the relatively smaller quantity of paramagnetic material present, the weaker intensities, marked 'P' in table 2, were eliminated from the spectrum of the magnetic fraction. Most of the remaining rings and their intensities correspond to the reflections of magnetite.

The *d*-values observed for synthetic magnetite were compared with those reported by Rooksby [3], for magnetite ($a = 0.839$ nm). Complete agreement for both lattice spacings and estimated intensities was obtained. These *d*-values are also listed in table 2. The *d*-values of the magnetic fraction are slightly larger than those of magnetite due to the larger lattice parameter ($a = 0.844$ nm).

The *d*-values of the γ-$FeMnO_3$ defect spinel were also compared with those of γ-Mn_2O_3 [7].

4. Discussion

The quadrupole splittings observed for both the magnetic fraction and the synthetic magnetite shown in table 1(*b*) are, within the error of the measurements, zero. This result implies that the Fe site symmetries are cubic.

The *d*-values of the magnetic fraction are similar to those of magnetite, after eliminating the weak paramagnetic values, and they also have the usual intensities.

The linewidth of the A site sextets is relatively narrow compared with that of the B sites. The broadening of the latter is ascribed to the existence of different Fe–Mn neighbour combinations giving rise to several overlapping peaks. This implies that the Mn ions occupy primarily octahedral sites. Sawatzky *et al* identified four different B peaks in $MnFe_2O_4$ at 298 K [8]. In the latter case the peak intensities are inverted with intensity of A $\ll$ intensity of B.

The respective magnitudes of the hyperfine magnetic fields are similar to each other (table 1) and are also not too dissimilar from those of natural magnetite which are 49.1 and 45.3 T for A and B sites at room temperature, respectively [9].

The change in hyperfine fields with change of Mn substitution has been measured by several investigators, [1, 10–12]. When plotted these points suggest a linear change in H with Mn content. Using this relation the composition of Mn and of the remaining Fe in the magnetic fraction have been approximated to $Mn_{0.6}Fe_{2.4}O_4$.

Comparison of the hyperfine fields of synthetic and natural magnetite reveals only a small difference between them. This difference is smaller than that observed for the magnetic fraction compared with the synthetic magnetite suggesting the presence of some impurities in the synthetic magnetite. The x-ray spectrum does not, however, show any impurity peaks from which to identify such impurities. The ME spectra on the other hand have the broadened octahedral peaks and the smaller intensity of the B peaks relative to the A peaks observed in the Mn-substituted material. Some foreign material is therefore believed to be present in the synthetic magnetite.

The quadrupole splittings of the paramagnetic component are considerably larger than expected for FCC spinels. Defect spinels have a metal ion vacancy in every three unit cells (see e.g., [1]). The large quadrupole splittings may be a consequence of changed symmetries due to Mn near neighbours of the Fe ions and to the presence of vacancies.

Isomer shifts are practically identical for the two doublets. On fitting one doublet to the spectrum (not shown) a width of 0.52 mm s^{-1} was measured. Not all the data points were reached by the theoretical curve obtained and X^2 was 2. On fitting two doublets X^2 was reduced to 1.7 and the fit to the innermost data points in the spectrum improved. The two halfwidths were then similar to the typical experimental values of 0.192 mm s^{-1} for Fe at 14 keV [13]. Two different sites are expected for a defect spinel which must

have both tetrahedral and octahedral sites. Two doublets are justified by the resolution obtained and by this requirement.

The A and B sublattices in γ-Fe_2O_3 which is magnetically ordered at room temperature can only be resolved in an applied field of 1.7 T [14].

The *d*-values of the paramagnetic component are similar to those of γ-Fe_2O_3 in which extra reflections, forbidden by space group extinction for FCC structures, appear [3]. Although similar they are consistently larger. These larger *d*-values are closer to those reported for γ-Mn_2O_3 (as listed in table 2) which is hexagonal with $c/a = 1.16$ ($a = 0.815$ nm, $c = 0.944$ nm), [7]. Reflections from this compound do not in general correspond to magnetite reflections. Substituting Mn for some of the Fe ions in γ-Fe_2O_3 would result in changes in the structure factor of γ-Fe_2O_3.

5. Conclusions

The main difference between the magnetic fraction and synthetic magnetite is the isomer shift of the octahedral sites which is larger in synthetic magnetite. The effect of this on the spectrum is evident in figure 1(*d*) where the right half of the sextet is relatively unresolved whereas the left half distinctly shows partially superimposed peaks.

The components in the uncalcined Fe–Mn–O powder are identified as a defect spinel γ-$FeMnO_3$, and as a Mn substituted magnetite with the approximate formula $Mn_{0.6}Fe_{2.4}O_4$. The former result confirms the identification made by Kolk *et al* [1, 2]. The latter represents a modification of the original identification of the magnetic phase as a Mn-substituted defect spinel.

The measured diffraction pattern has provided information on detailed differences in intensities of reflections from those of both magnetite and of γ-Fe_2O_3. The lattice parameter $a = 0.844$ nm has also been determined for both components assuming cubic structures.

The ME spectra of both the synthetic magnetite and the magnetic component suggest that the site occupations differ from those of the Mn-rich magnetite. The latter has less intense A sites than B sites although the B sites are broad in all cases under discussion. The implication of this is that Mn in Mn-poor materials occupy octahedral sites predominantly whereas tetrahedral sites are also filled by Mn in Mn-rich materials. The cause of the different peak ratios of the B sites, where the innermost peak intensities of the octahedral sextet are two-thirds of those of the two outer peaks, is still unknown.

Acknowledgments

The author acknowledges with thanks the assistance of Mr G R Hearne of the Mössbauer Laboratory, Mrs J Salemi for the x-ray measurements and Dr I R Leith of the National Institute of Chemical Engineering Research at the CSIR, Pretoria, who prepared and supplied the Fe–Mn–O powders. Grateful acknowledgments are also made to the National Energy Council for their sponsorship of this research.

References

[1] Kolk B, Albers A, Leith I R and Howden M G 1988 *Appl. Catal.* **37** 57

[2] Kolk B, Albers A, Hearne G R and le Roux H 1988 *Hyperfine Interact.* **42** 1051
[3] Rooksby H P 1951 *X-ray Diffraction of Clay Minerals* ed G W Brindley (London: The Mineralogical Society (Clay Mineral Group)) p 244
[4] Haul R and Schoon T 1939 *Z. Phys. Chem.* B **44** 216
[5] Verwey E J W and Haayman P W 1941 *Physica* **9** 979
[6] Maiti G C, Malessa R and Baerns M 1983 *Appl. Catal.* **5** 151
[7] Moore T E, Ellis M and Selwood P W 1950 *J. Am. Chem. Soc.* **72** 856
[8] Sawatzky G A, van der Woude F and Morrish A H 1969 *Phys. Rev.* **187** 747
[9] Greenwood N N and Gibb T C 1971 *Mössbauer Spectroscopy* (London: Chapman and Hall) p 241
[10] Hucl M K, Van der Woude F and Sawatzky G A 1972 *Phys. Lett.* **42A** 99
[11] Tanaka M, Mizoguchi T and Aiyama Y 1963 *J. Phys. Soc. Japan* **18** 1091
[12] Sawatzky G A, Van der Woude F and Morrish A H 1967 *Phys. Lett. (Netherlands)* A **25** 147
[13] Greenwood N N and Gibb T C 1971 *Mössbauer Spectroscopy* (London: Chapman and Hall) p 18
[14] Armstrong R J, Morrish A H and Sawatzky G A 1966 *Phys. Lett.* **23** 414